A Study of 5 Physical Double Star Systems

Katherine Lee[1], Jett Peters[1], Daniel Vurgaftman[1], Elle Moscinski[1], Justin Wang[1], Kalée Tock[1]
[1]Stanford Online High School, 415 Broadway Academy Hall, Floor 2, 8853, Redwood City, CA 94063

Abstract

The five double star systems, HJ 3262, STF 364, ES 889, HJ 3789, and STF 401AB were queried from the Washington Double Star Catalog (WDS) and analyzed to investigate the probability of a gravitational attraction within the system and the possibility of a trend in the relative motion of the stars. Three of the double stars were imaged with the Las Cumbres Observatory's 40-centimeter telescopes and two were measured with the Las Cumbres Observatory's PlaneWave DeltaRho telescope. Images were reduced with AstroImageJ and the position angles and the separations were measured. Previous measurements were used to create historical data plots for all the systems with python. Those plots, along with the value of the relative proper motion and the escape velocity calculated from the Gaia Data Release 3, suggest these systems all exhibit either common proper motion or similar proper motion. For two systems (HJ 3262 and HJ 3789), the stars are more than one light year apart making a gravitational relationship unlikely. For ES889 and STF364, there is a possibility that the pairs are gravitationally bound. Finally, for STF 401AB the evidence is insufficient to assess the likelihood of a gravitational relationship. Due to the high uncertainty, it is worth making additional measurements to shed further light on the nature of these systems.

1. Introduction

The stars for this study were selected based on the following criteria: the magnitude less than 13 so that they would be visible to the Las Cumbres Observatory Global Telescope (LCOGT) network 0.4-inch and PlaneWave DeltaRho telescopes, the difference in magnitude between stars of each pair less than 3 allowing both stars to resolve with the same exposure time, and the separation between 5 and 20 arcseconds in order to properly visualize stars within the separation range for our instruments. A potential result of these criteria is that the targets selected were all middle-range main sequence stars or red giants since red dwarfs tend to be faint and the relative frequency of type O or B stars is low. The stars' absolute magnitudes were calculated using $Mv = m + 5(logp + 1)$ where m is the apparent magnitude and p (mas) is the parallax, both collected from the Gaia Data Release (DR3) (Prusti et. al, 2016b; Vallenari et. al, 2022k). The colors of the stars in the system were extracted from DR3 or previous scientific literature about the star. The data were used to make estimates of the star's spectral type and luminosity using the Gaia Color Magnitude Diagram (CMD) shown below in Figure 1 which was then plotted on the Hertzsprung-Russell (HR) Diagram shown below in Figure 2. This was then used to estimate the star's mass as shown below in Table 2 (Babusiaux et. al., 2018). Mass estimates for the primary in ES 889 and the primary and secondary in the HJ 3789 system were especially difficult to approximate due to the high variation in masses of red giant stars, though spectral types determined in previous papers were useful in narrowing the range of possibilities (Hagen and Stencel, 1985). Furthermore, both stars in HJ 3789 have been classified as being in the Red Clump making them standard candles and therefore of great use in distance measurements beyond the parallax range (Ruiz-Dern et al., 2018). For the system HJ 3262, mass estimates exist in previous literature and are reproduced here (Cruzablebes, P. et al).

To plot stars on an HR diagram, two pieces of information are needed: the luminosities of the stars in solar units, and the spectral types of the stars. The Gmag of the star was obtained from Gaia DR3, and this

number was corrected with the DR3 parallax measurement to give the absolute magnitude of the star. Using the following equation, the luminosity was calculated.

$$M = -2.5 \log_{10} \left(\frac{L}{L_0} \right)$$

In this formula, M represents absolute magnitude, L represents luminosity, and L_0 represents the zero-point luminosity, which is equal to 3.0128×10^{28} W. For example, the primary star in the HJ 3262 system has an absolute magnitude of 1.00. If this value is calculated using the above equation, the output is a number of watts equivalent to 31.33 solar luminosities.

The second piece of information is the Gaia RP - BP color. This value can be obtained from Gaia DR3 and can be used, in conjunction with the diagram below, to infer the spectral type of the star. For example, the primary star in HJ 3262 has an RP - BP value of 1.19, as seen in Table 1. From the diagram, we can infer that it is a G-type star. With these two pieces of information, the star can be plotted on an HR diagram, as shown in Figure 2.

Table 1: Gaia Color and Magnitude Data

Star System	Gaia RP - BP Color (P)	Gaia RP - BP Color (S)	Gaia Absolute Magnitude (P)	Gaia Absolute Magnitude (S)
HJ 3262	1.19	0.81	1.00	2.35
STF 364	0.55	0.55	2.98	3.18
ES 889	1.51	0.99	0.81	3.93
HJ 3789	1.22	0.70	1.81	2.43
STF 401	0.03	0.11	1.55	1.92

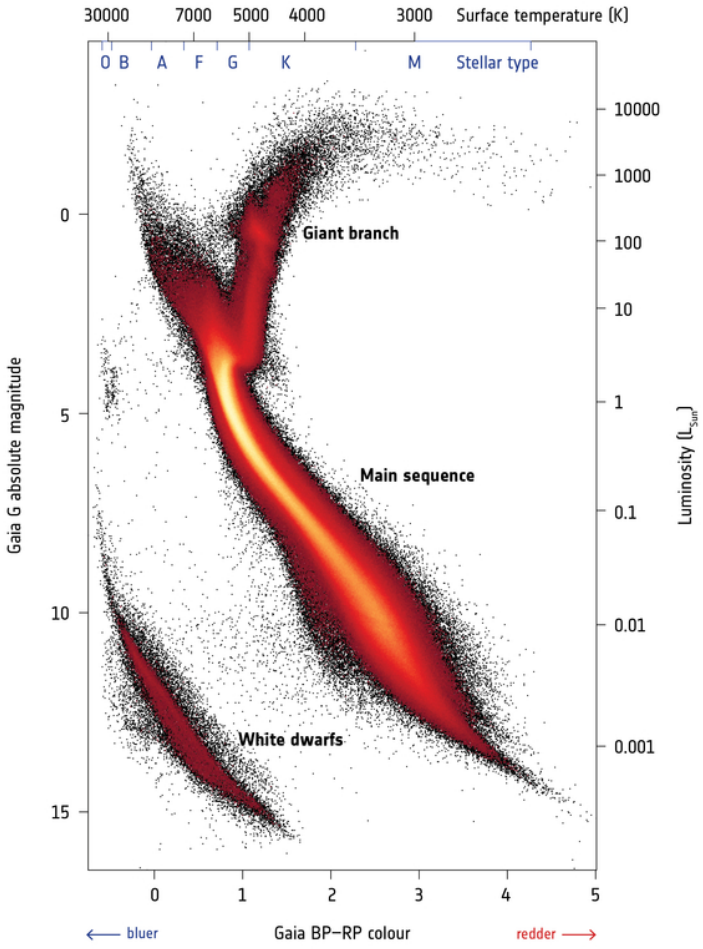

Figure 1: Gaia HR diagram

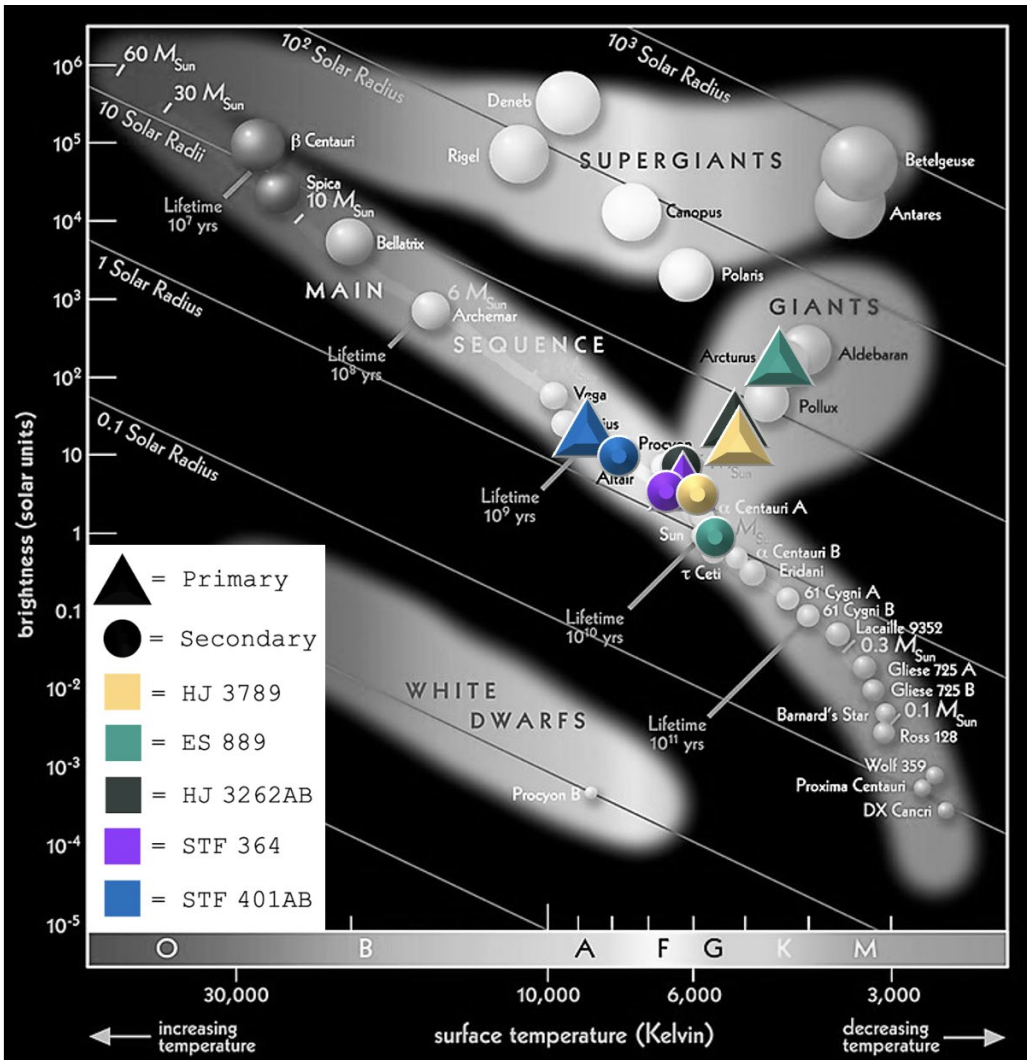

Figure 2: HR diagram of the 10 analyzed primary and secondary stars

Table 2: Primary Star and Secondary Star's Solar Masses ($M_\odot$) and Spectral Class; Classified red giants are denoted with an asterisk (*)

Star System	Constellation	Primary Star $M_\odot$	Secondary Star $M_\odot$	Primary Star Spectral Class	Secondary Star Spectral Class
HJ 3262AB	Orion	0.7	1.5	G*	F
HJ 3262AC	Orion	0.7	0.5	G*	K
STF 364	Perseus	1.0	1.5	F	F
ES 889	Auriga	3.0	1.4	K*	G
HJ 3789	Pictor	1.5	1.1	G3*	G3*
STF 401	Taurus	2.1	1.9	A	A

2. Instruments Used

The instruments used for three of the measurements discussed in this paper (HJ 3262, STF 364, HJ 3789) were Las Cumbres Observatory's 40-centimeter telescopes. These telescopes are equipped with a PanSTARRS-W filter and an SBIG STL-6303 CCD sensor. The Las Cumbres Observatory has ten 40-centimeter telescopes located in different places around the world, and one of LCOGT's 40-centimeter instruments can be seen in Figure 3. The telescopes are wholly modified Meade 16" telescopes, using a modified Schmidt-Cassegrain design with a focal length of 3251 mm. The Schmidt-Cassegrain design is a hybrid-optical system that utilizes a glass corrector plate and a pair of spherical mirrors. The path of light begins by refracting through the glass corrector plate, followed by reflection off the primary mirror, then off the secondary mirror before passing through a hole in the primary, ultimately striking the camera or eyepiece. The camera attached to these scopes is the SBIG STL-6303, which uses the KAF-6303E/LE CCD chip with a pixel array of 2048 by 3072 9-µm pixels, meaning that the sensor is 27.7 mm by 18.5 mm. Combining the telescope and camera gives a field of view (FOV) of 0.32° by 0.49° with a resolution of 0.57" per pixel. The measurements for the other two systems (STF 401AB, ES 889) were taken from images captured by the Las Cumbres Observatory's PlaneWave DeltaRho telescope located at the Haleakala Observatory, which is equipped with a PanSTARRS-W filter and a QHY 600 CMOS sensor. The DeltaRho telescope is a 350 mm Corrected Dall-Kirkham design with a focal length of 1050 mm and an F-number of 3. The QHY600 is a full-frame camera with a pixel array of 9576 by 6388 (61.2 MP). The QHY 600 combined with the PlaneWave DeltaRho produces a FOV of 1.3 degrees by 1.96 degrees. This system has a resolution of 1.5" per pixel. A picture of The DeltaRho telescope is shown in Figure 4.

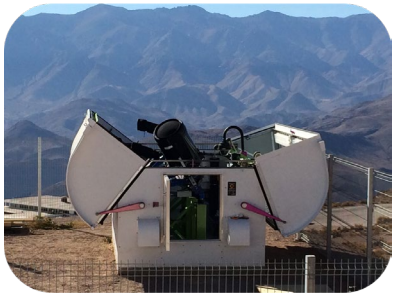

Figure 3: LCOGT 40-Centimeter in Chile

Figure 4: LCOGT PlaneWave DeltaRho

3. Measurement

The images collected from the telescopes discussed in the previous section were resolved cleanly, despite some slight saturation of STF 401AB. A point spread function of each of the five double stars can be seen in Figure 5. All three stars in the triple system HJ 3262 are noted to be apparent on the point spread function

surface plot with the presence of three peaks in relatively close proximity to each other. The images returned from LCOGT were processed using AstroImageJ (AIJ). Although some of the stars were slightly asymmetric, AIJ's computed centroid was at the visual center of each star, as shown in Figure 6. The shapes of the stars in systems HJ 3789 and ES 889 suggest a possible slight tracking irregularity.

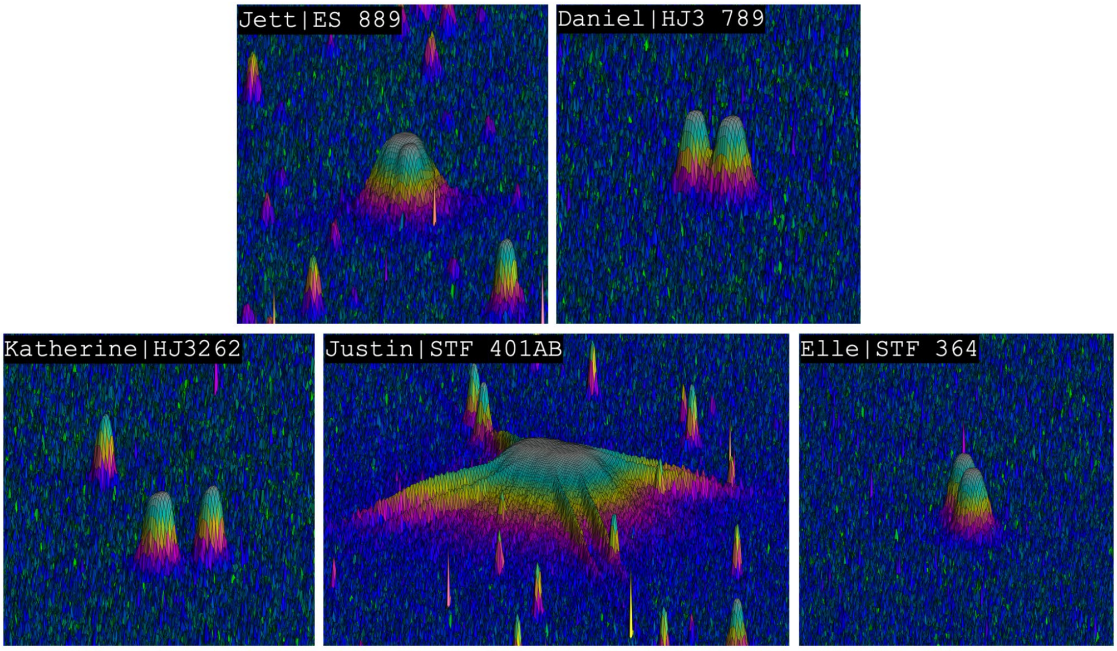

Figure 5: Point spread functions for each of the 5 double stars; ES 889 and STF 401AB are taken with the Delta Rho telescope; HJ 3789, HJ 3262, and STF 364 with the 0.4-meter telescopes

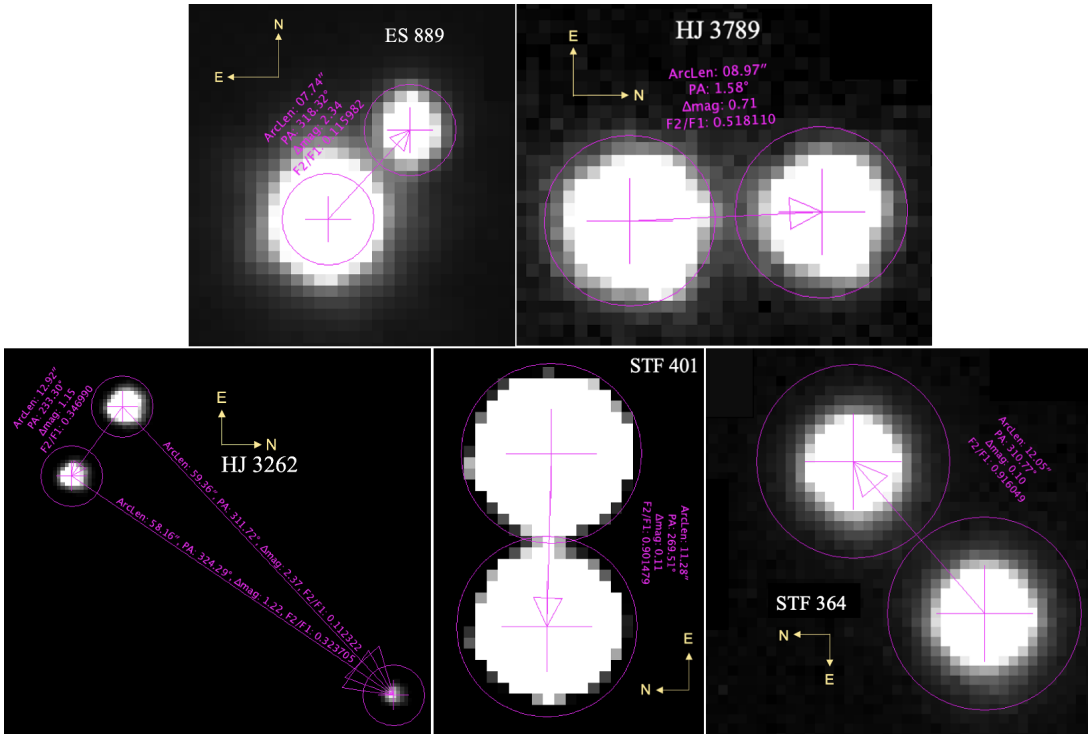

Figure 6: Images of measurements for each of the 5 double stars in AstroImageJ

4. Results

Both the position angle and separation are an average of the 10 LCOGT image measurements done in AIJ shown below in Table 2. The measurement aperture used in AIJ is also reported.

Table 2: Measurements made in January 2023

System	Date:	Number of Images	Position Angle (°)	Standard error on PA	Separation (")	Standard Error on Sep	Measurement Aperture (px)
HJ 3262AB	2023.020	10	233.1	±0.03	23.89	±0.01	7
HJ 3262AC	2023.020	10	311.8	±0.02	59.33	±0.01	7
HJ 3262BC	2023.020	10	324.3	±0.02	58.21	±0.02	7
STF 364	2023.040	10	310.7	±0.02	11.95	±0.01	10
ES 889	2023.059	10	317.8	±0.08	7.68	±0.00	4
HJ 3789	2023.016	10	1.6	±0.06	8.94	±0.06	7
STF 401AB	2023.061	9	269.2	±0.19	11.29	±0.01	8

The system escape velocity can be calculated with the given formula:

$$V_{escape} = \sqrt{\frac{2G(m_1 + m_2)}{r}}$$

where $m1$ and $m2$ are the masses of the primary and secondary stars in kilograms, respectively, r is the distance between the two stars in space (2D distance if the parallax uncertainties overlap, and 3D distances otherwise), and G is the gravitational constant, $6.67 \times 10^{-11} (m^3)/(kgs^2)$. If the relative space velocity is greater than the system escape velocity, it could suggest the double stars are not gravitationally bound. The calculated escape velocities for each pair are shown below in Table 3. Based on these data, we can conclude with some confidence that the systems HJ 3262 and HJ 3789 are not bound, while the systems ES 889 and

STF 364 have a rather high probability of being bound. However, for the system STF401AB, we cannot make any conclusion with a high level of confidence.

Table 3: Estimated values for 2D or 3D relative space velocity and escape velocity derived from Gaia data. Stars for which the 2D relative velocity was used are marked with an asterisk (*).

System	Estimated 2D or 3D Relative Space Velocity (m/s)	Estimated 3D Escape Velocity (m/s)
HJ 3262AB	1343	21
HJ 3262AC	38069	22
STF 364	788*	1825
ES 889	700*	1400
HJ 3789	1000	109
STF 401AB	3728*	2457

The proper motion, parallax, rPM, and proper motion classification are shown in Table 4. The rPM (proper motion ratio) can be used to characterize the degree of similarity of the proper motions of a pair of stars. It is given by relative proper motion divided by the longest proper motion vector (Harshaw, 2016). Thus, the numerator of the ratio is given by $\sqrt{(R1-R2)^2+(D1-D2)^2}$ where $R1$ and $R2$ are the proper motion in right ascension of the primary and secondary star, respectively, and $D1$ and $D2$ are the proper motion in declination of the primary and secondary star, respectively. The denominator of the rPM is the magnitude of the greater PM vector between the primary and the secondary. In the case of HJ 3262AB, the rPM of 0.387 is within the range of 0.2 - 0.6 meaning it has a similar proper motion (SPM). HJ 3262AC and HJ 3262BC display rPM greater than 0.6 and are therefore classified as having different proper motions (DPM). Stars STF 364, ES 889, HJ 3789, and STF 364AB all exhibit common proper motion (CPM) with the rPM between the range 0 - 0.2, indicating the stars are moving together in space.

Table 4: Parallax for both primary and secondary systems in milliarcseconds, proper motion for both primary and secondary systems in milliarcseconds per year (RA, Dec), rPM, and classification.

System	Parallax of Primary (mas)	Parallax of Secondary (mas)	Proper Motion of Primary (mas/year)	Proper Motion of Secondary (mas/year)	rPM	Classification
HJ 3262AB	2.12±0.09	2.32±0.02	(-0.96±0.1, -1.22±0.08)	(-0.36±0.02, -1.19±0.02)	0.387	SPM
HJ 3262AC	2.12±0.09	2.22±0.02	(-0.96±0.1, -1.22±0.08)	(16.04±0.1, -2.17±0.02)	1.052	DPM
HJ 3262BC	2.32±0.02	2.22±0.02	(-0.36±0.02, -1.19±0.02)	(16.04±0.03, -2.17±0.02)	1.015	DPM
STF 364	7.33±0.02	7.2±0.02	(31.06±0.02, -41.1±0.02)	(30.54±0.02, -41.01±0.02)	0.010	CPM
ES 889	2.259±0.01	2.257±0.01	(15.88±0.016, -35.82±0.01)	(15.55±0.02, -35.89±0.01)	0.008	CPM
HJ 3789	5.20±0.02	5.15±0.02	(4.44±0.02, 20.24±0.02)	(4.55±0.03, 20.28±0.03)	0.006	CPM
STF 401AB	9.71±0.04	9.69±0.04	(38.86±0.06, -30.56±0.05)	(38.25±0.04, -31.99±0.03)	0.031	CPM

5. Plots

With no previous orbital solution for any of the five systems, historical data from the Washington Double Star Catalogs was plotted with respect to time using python and matplotlib as shown below in Figure 7. Yellow and red markings represent the older measurements, documented between the early 19th century to the early 20th century with measurement tools such as the micrometer. Green markings represent the earlier measurements taken with instruments such as Gaia and CCD imaging. Of these, the green darker colors represent the newest measurements and green lighter colors are the oldest.

At first glance, the plot corresponding to the relative motion of HJ 3262AB's secondary star is suggestive of some sort of orbital motion, not around the primary star, but instead potentially around an invisible companion such as a white dwarf or neutron star. However, this is unlikely as the points are only within an arcsecond of each other, which is beneath the noise floor of the measurements. Similarly, HJ 3262AC does not exhibit any trend of orbit. The B and C stars of the HJ 3262 system have not previously been measured relative to each other. STF 364 also does not display a visible trend around the primary star at the origin which suggests the stars are gravitationally bound and orbiting each other. ES 889's secondary star appears to be moving towards the primary star with respect to time, but the data available are not sufficiently definitive to assess the nature of this movement. The earliest three points, taken in 1910, 1922, and 1991, are likely outliers while the rest of the data points remained relatively closer together, corroborating the accuracy of the most recent measurement. The measurements of HJ 3789 are consistent with previous historical data, although the overall movement with respect to time remains unclear since a 2016 measurement overturned a previous trend of movement towards 0 arcseconds of RA relative to the primary.

The measurement made here does not restore that trend, although a clearer picture of the relative motion may be obtained through future astrometric assessments. The plot of STF 401AB does not reflect a trend over time. While the earliest measurement in 1777 is an outlier and the most recent measurements are within a similar range, there is little visible coordination of the secondary star's orbit with regard to time.

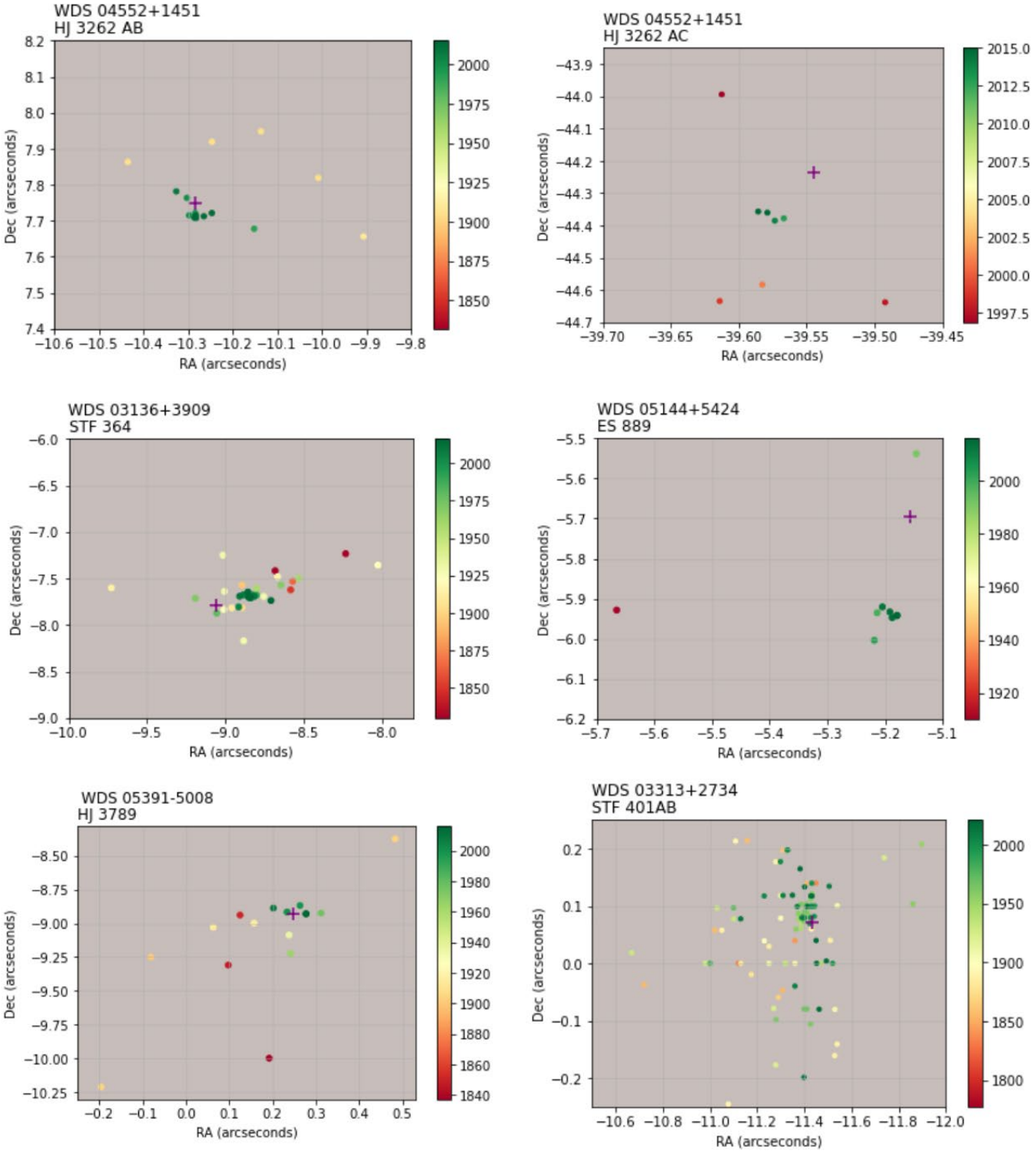

Figure 7: Historic Data Plot of Stars (minor outliers have been omitted)

6. Discussion

None of these stars had a previously suggested orbital solution, but the measurements largely landed close to the most recent measurements. To investigate whether a gravitational relationship would be expected to be apparent from the historical plots, the orbital period in years was estimated with Kepler's 3rd law:

$$\sqrt{r^3/m}$$

where r is the transverse separation in astronomical units (or 3D spatial separation if parallax uncertainties do not overlap) and m is the mass of the primary star in units of solar masses. The various orbital periods for the stars are shown in Table 5 below. No orbital period calculation was performed for the stars HJ 3282 and HJ 3789 because their 3D spatial separation exceeded 1 light year, causing them to be unlikely to be observable as bound (Nugent, 2022).

Table 5: Orbital Period of System (if allowed)

System	Orbital Period (years)
STF 364	≈53,906
ES 889	≈119,869
STF 401AB	≈27,743

The orbital period may explain the need for prolonged observation to visualize the orbit of the secondary around the primary star if the pairs were to be gravitationally bound. Movement of the secondary star in systems ES 889, STF 364, and STF 401AB would be expected to display almost no movement in the few hundred years that measurements have been taken, and therefore, continued observations on a larger time scale could sufficiently resolve uncertainty present over orbital periods.

a) HJ3262AB/AC/BC
   For this triple system, all three pairs of stars have a 3D spatial separation of greater than 1 light year (this number being outside of measurement uncertainty). Moreover, for the AB pair, the parallax uncertainty does not overlap and the estimated relative motion greatly exceeds the estimated escape velocity in the system. While some degree of uncertainty remains on the velocity estimates, the distance measurements as well as the velocity approximations and rPM suggest that the AB pair star system is merely physical and does not represent a gravitational relationship. Meanwhile, the rPM value for the AC and BC part of the system is greater than 1, suggesting that those pairs do not even represent physical doubles.

b) STF364
This double's 3D spatial separation value from Gaia DR3 data is greater than 1 light year but, the level of uncertainty on the measurement is sufficient to reduce the 3D separation to less than 1 light year. The parallax uncertainties overlap and the measured 3D velocity is a factor of 2 less than the estimated escape velocity. Previous papers have suggested that a difference of a factor of 4 to 5 between the escape velocity and the 3D velocity is needed to make a conclusion about the gravitational relationship between the stars (Caputo et. al., 2020). However, with the improved accuracy of the data in Gaia DR3, the difference here is sufficient to at least suggest a relatively high probability of these stars being gravitationally bound. The two stars in this double have a similar color, which could indicate similar chemical composition, making this star a potential object of interest for continued study.

c) ES 889
Meanwhile, for this double, the 3D spatial separation value from DR3 data is greater than 1 light year. The level of uncertainty on the parallax measurement is again sufficient to put the double into a 3D distance of less than 1 light year. The parallax uncertainty means that the stars' distance ranges overlap, meaning they might be the same distance from Earth. If we assume that the two stars are the same distance in the radial direction then the 3D separation shrinks to 0.017 pc. In addition, the measured 3D velocity is more than a factor of 2 less than the estimated escape velocity. As for the previous star, the difference factor is not quite high enough to make an absolute conclusion, but it is sufficient to suggest that the stars are bound to a significant probability. The plot of the historical measurements of this double star, as seen in Figure 6, does not show any definitive trends. However, this could be due to the long orbital period of the system. As seen in Table 5, the orbital period based on the mass estimate made previously, is over 100,000 years. This means further measurements over a much longer timescale would be necessary in order to see trends.

d) HJ 3789
This double's 3D spatial separation is greater than 1 light year, which is outside of the measurement uncertainty. The parallax uncertainties on the two stars do not overlap as well. Moreover, the relative motion of the stars exceeds the system escape velocity in the system by a factor of 100. While uncertainty remains on the velocity estimates, particularly in the value for the radial velocity of the secondary, the distance measurements suggest that this triple star system is merely physical and does not have a gravitational relationship.

e) STF 401AB
This double has a measured 3D spatial separation of less than one light year, although the measurement uncertainty is too high to make any specific conclusions from this. While the escape velocity of 2457 m/s is a factor of 1.5 lower than the 3D space velocity of 3728 m/s, it is not quite sufficient to make definitive conclusions regarding this system, so additional measurements of the stars will be necessary to make a clearer determination as to the likelihood of a gravitational relationship.

While there is no visible curvature in the historic data plots (Figure 6), there are suggestions that the stars are not moving in a certain direction away from each other and instead are moving together in space. The plot may instead imply that the stars have originated from the same gas cloud, cluster, or nebula, and were ejected in the same direction at the same time.

7. Conclusion

The measurements presented in this study are within what is expected based on previous historical measurements. HJ 3262 AB and HJ 3789 AB are likely to be unbound doubles, while for the remainder, the existence of a gravitational relationship is suggested but cannot yet be conclusively determined. Continued observations and measurements such as those presented here will make more accurate classifications possible for all these systems.

Acknowledgments

This research was made possible by the Washington Double Star catalog maintained by the U.S. Naval Observatory, the Stelledoppie catalog maintained by Gianluca Sordiglioni, Astrometry.net, AstroImageJ software which was written by Karen Collins and John Kielkopf, and PixInsight developed by Pleiades Astrophoto. This paper contains plots constructed using PixInsight software.

This work has also made use of data from the European Space Agency (ESA) mission Gaia (https://www.cosmos.esa.int/gaia), processed by the Gaia Data Processing and Analysis Consortium (DPAC, https://www.cosmos.esa.int/web/gaia/dpac/consortium). Funding for the DPAC has been provided by national institutions, in particular, the institutions participating in the Gaia Multilateral Agreement.

This work makes use of observations taken by the 0.4m telescopes of Las Cumbres Observatory Global Telescope Network located in Haleakala Hawaii, USA, Tenerife, Spain, and Cerro Tololo, Chile.

References

Caputo, R. et. al (2020). Observation and Investigation of 14 Wide Common Proper Motion Doubles in the Washington Double Star Catalog. Journal of Double Star Observations, 16(2), 173–182. http://www.jdso.org/volume16/number2/Caputo_173_182.pdf

Cruzalèbes, P. et al. (2019). A catalog of stellar diameters and fluxes for mid-infrared interferometry. Monthly Notices of the Royal Astronomical Society, 490(3), 3158–3176. https://doi.org/10.1093/mnras/stz2803

Hagen, Wendy and Stencel, Robert E, 1985. "On the Rarity of FK Com Stars", *The Astronomical Journal* **90** (1), 120-122.

Harshaw, Richard (2016). CCD Measurements of 141 Proper Motion Stars: The Autumn 2015 Observing Program at the Brilliant Sky Observatory, Part 3. Journal of Double Star Observations, 12(4), 394–399. http://www.jdso.org/volume12/number4/Harshaw_394_399.pdf

Gaia Collaboration, C. Babusiaux, F. Van Leeuwen, et al. (2018). Gaia Data Release 2: Observational Hertzsprung-Russell diagrams. *A&A* **616**, A10. https://www.aanda.org/articles/aa/full_html/2018/08/aa32843-18/aa32843-18.html

Gaia Collaboration, T. Prusti, J.H.J. de Bruijne, et al. (2016b). The Gaia mission. A&A 595, A1. https://www.aanda.org/articles/aa/full_html/2016/11/aa29272-16/aa29272-16.html

Gaia Collaboration, A. Vallenari, A. G. A. Brown, et al. (2022k). Gaia Data Release 3: Summary of the content and survey properties. arXiv e-prints, https://arxiv.org/abs/2208.00211

Nugent, R., 2022. Optical or Binary? An Investigation of 21 WDS Systems. Journal of Double Star Observations, 18(1), 41-51. http://www.jdso.org/volume18/number1/Nugent_41_51.pdf

Ruiz-Dern, L., Babusiaux C., et. al. "Empirical Photometric Calibration of the *Gaia* Red Clump: Colours, effective temperature, and absolute magnitude". *A&A* **609**, A116. https://www.aanda.org/articles/aa/pdf/2018/01/aa31572-17.pdf